Summer 2001

Encoding and storage components of verbal working memory as revealed by a factorial design, an FMRI study

Jason Steffener
New Jersey Institute of Technology

ABSTRACT

ENCODING AND STORAGE COMPONENTS OF VERBAL WORKING MEMORY AS REVEALED BY A FACTORIAL DESIGN, AN FMRI STUDY

by
Jason Steffener

In this fMRI study, the contributions of frontal and posterior brain regions to verbal working memory were investigated. A two-factor design with low and high memory load (2 and 5 letters) and short and long delay (4 and 12 secs.) as factors were used. Based on reports in the literature, we expect activity in the following frontal and parietal brain regions of interest (ROIs): Brodmann areas (BA) 6, 9, 46, 44, 45, 7 and 40. The analysis of collected fMRI data involved image processing and statistical analysis methods including realignment, spatial normalization, spatial smoothing, temporal filtering, intensity normalization, statistical tests, and thresholding of results. The design allowed for testing the interaction and main effects of the two factors. The interaction terms revealed involvement in the caudate and BA 6, 9, and 7. The main effects revealed activity in BA 6, 9, 32, 40, 44, cerebellum, thalamus, and caudate. The results of this study support the literature and offer more insight into previous findings.

ENCODING AND STORAGE COMPONENTS OF VERBAL WORKING MEMORY AS REVEALED BY A FACTORIAL DESIGN, AN FMRI STUDY

by
Jason Steffener

A Dissertation
Submitted to the Faculty of
New Jersey Institute of Technology
in Partial Fulfillment of the Requirements for the Degree of
Master of Science in Biomedical Engineering

Department of Biomedical Engineering

August 2001

APPROVAL PAGE

ENCODING AND STORAGE COMPONENTS OF VERBAL WORKING MEMORY AS REVEALED BY A FACTORIAL DESIGN AN FMRI STUDY

Jason Steffener

Dr. H. Michael Lacker, Thesis Adviser **Date**

Professor of Biomedical Engineering, NJIT

Dr. Stanley Reisman, Committee Member **Date**

Professor of Biomedical Engineering, NJIT

Dr. Benjamin M. Bly, Committee Member **Date**

Assistant Professor of Psychology, Rutgers Newark

BIOGRAPHICAL SKETCH

Author: Jason Steffener

Degree: Master of Science

Date: August 2001

Undergraduate and Graduate Education:

- Master of Science in Biomedical Engineering,
  New Jersey Institute if Technology, Newark, NJ, 2001

- Bachelor of Science in Applied Physics,
  New Jersey Institute of Technology, Newark, NJ, 2000

Major: Biomedical Engineering

Presentations and Publications:

Lange, G. , Holodny, A., DeLuca, J., Lee, H.J., Yan, X.H.M., Steffener, J., Natelson, B.H., "Quantitative Assessment of Cerebral Ventricular Volumes in CFS," Applied Neuropsychology 2001;8(1):23-30

Christodoulou C., DeLuca, J., Ricker, H.J., Madigan, N., Bly, B.M., Lange, G., Kalnin, A.J., Liu, W.-C., Steffener, J., Diamond, B. and Ni, A.C., "Functional magnetic resonance imaging of working memory impairment following traumatic brain injury," Journal of Neurology, Neurosurgery and Psychiatry 2001;71:161-168 (August)

Steffener, J., Bly, B.M., Janal, M., Lange, G., "Encoding and storage components of verbal working memory as revealed by a factorial design," NeuroImage 2001;13(6):S744

Lange, G., Steffener, J., Christodoulou, C., Liu, W.-C., Bly, B.M., DeLuca J., Natelson, B.H., "FMRI of auditory verbal working memory in severe fatiguing illness," NeuroImage 2000;11(5):S95

DEDICATION

This thesis is dedicated to three important people. First, Dr. Gudrun Lange. She has done so much to help me grow and develop professionally. Without her support, encouragement and guidance this project would not have been possible. I owe her more thanks than I can write here.

Second, my mother. She has always been supportive of any path I thought of taking. I hope I have chosen one that also makes her proud.

Finally, Florence Jaouen. Her support of me through this project has been essential to its completion. I appreciate all she has done for me and am forever grateful.

ACKNOWLEDGMENTS

The author wishes to thank his advisor, Professor H. Michael Lacker, for his support and insight into this project.

Special thanks to Professors Stanley Reisman and Benjamin M. Bly for serving as members of the committee.

The author appreciates all the support and suggestions during the development of this project form Drs. Gudrun Lange and Dane Cook.

Dr. Wen-Ching Liu was essential to this project for his ability to scan the subjects.

TABLE OF CONTENTS

TABLE OF CONTENTS

(CONTINUED)

LIST OF TABLES

LIST OF FIGURES

CHAPTER 1

INTRODUCTION

Working memory (WM) is the cognitive process underlying the temporary storage and manipulation of information [1]. Baddeley proposed a working memory model consisting of three components, the central executive, the visuospatial sketchpad, and the phonological loop. The phonological loop is thought to be responsible for storing and retaining verbal information in a temporary storage buffer via subvocal rehearsal. The central executive component is thought to manipulate this information for further information processing (i.e., decision to respond to a cue using verbal information stored in WM). The information in phonological storage decays within one to two seconds, therefore there is the need for constant rehearsal via articulatory speech processes[2].

In a recent review of neuroimaging studies, Smith et al. [3] summarize research findings describing a neural architecture that may underlie Baddeley's [1] model of verbal working memory. They conclude that previous research suggest the subvocal rehearsal component of verbal WM appears to be sub served by left-hemisphere frontal speech regions, including Broca's area in the inferior frontal gyrus (Brodmann Area 44), the inferior aspect of the precentral gyrus in Brodmann Area 6, and the supplementary motor cortex within the superior portion of Brodmann Area 6. The left posterior parietal cortex (Brodmann Area 40) mediates a storage buffer, while the dorsolateral prefrontal cortex (Brodmann Area 9/46) is thought to mediate the executive component of the verbal working memory system. The primary goal of this fMRI study was to reveal significant signal change in the neural correlates of encoding and storage of verbal working memory using a factor analytic approach.

CHAPTER 2

BACKGROUND

2.1 Task Background

Recently, two types of tasks were used to place demands on the working memory system to dissociate the rehearsal component of verbal WM from the storage component. These two tasks are the n-back task and the item recognition task. The n-back task involves sequential presentation of items to be held in the temporary storage buffer and is designed to increase demands on the maintenance of the memory trace by increasing the load, the number of items to retain. With an increase in the memory load comes an increase in the time it takes to subvocally rehearse this information so it can be retained in the storage buffer [4, 5]. Thus, increases in brain regions associated with this task can be attributed to either the effect of load or length of rehearsal period since these components are confounded. Regional significant signal change in response to this task may be due either to the increase in load or the increase in rehearsal period.

The item recognition task is a task where items are presented to the subject in a block, following a delay period the subject determines whether a single probe item was in the initial block of items. This task allows for a possible dissociation of the two factors hypothesized to constitute the phonological loop -- the number of items in the initial presentation and the length of delay. Varying the number of items presented in the initial block is a variation of the memory load [6]. The length of the rehearsal period for items held in memory is changed with variation in the delay period between item presentation and probe presentation. [7].

Multiple variations of these two methods have been used to tease apart the neural components of verbal working memory each with their own strengths and weaknesses. Cohen et al. 1997 [8] used a parametric variation of the n-back task to look for a dissociation of storage and rehearsal components. The main effect of load (i.e. an increasing number of sequentially presented items to remember) revealed increased activation in Broca's Area (BA44), posterior parietal cortex and the dorsolateral prefrontal cortex (DLPFC). The interaction between the rehearsal period and load was revealed in increases in signal change in Broca's Area and the posterior parietal regions. They propose that this interaction may be associated with updating the contents of the storage buffer during rehearsal. Braver et al. [4] corroborated Cohen et al.'s finding of the effect of load using a similar parametric paradigm design.

Rypma et al. 1999 [6] used an item recognition task to avoid the confound of delay and load by varying the task load and keeping the delay constant. The authors used this design to determine if the executive component of working memory would be activated with an increase in memory load. Their findings included activations in bilateral inferior frontal gyri, including Broca's Area, bilateral posterior parietal regions and caudate nucleus.

Barch et al. 1997 [7] also used the item recognition task; however, they varied the task along the rehearsal period. The question of their study was whether an increase in working memory demand, in the form of a longer rehearsal time, causes an increase in DLPFC activation. This experiment revealed activation in the DLPFC, Broca's Area and the left posterior parietal region.

Using these different tasks the studies presented show a large amount of overlap in their findings. The four studies all showed activation in the left inferior frontal gyrus, Broca's Area, thought to be involved in sub-vocal rehearsal [3]; with three of these showing activation in the right hemisphere as well. Three of the studies showed activation in the precentral gyrus, also thought to be involved in sub-vocal rehearsal, the study by Barch et al. did not show this result. All four of the studies showed response in the storage buffer of the left posterior parietal cortex with the two n-back tasks also demonstrating right hemisphere responses. The hypothesized location for the executive functions of working memory, the DLPFC, was responsive bilaterally for Braver et al., left sided for Barch et al. and right sided for Cohen et al.'s experiment.

The experiments above look for the effects on the working memory system with the manipulation of one slave system subcomponent. However, only Cohen et al. address the interaction of one subcomponent of verbal WM with another, how one-slave system subcomponent changes in the context of another. Their task however, does not directly manipulate the length of rehearsal period and therefore does not reveal the effects of an increased load over varied rehearsal periods. Table 1 summarizes these experiments and their findings. The table list the four studies described above and whether they found activation in the listed regions as well as the hemisphere.

TABLE 1 Summary of literature review

	Inferior Frontal Gyrus (BA 44)	Inferior Precentral (BA 6)	Superior Precentral (BA 6)	Parietal Cortex (BA 7 BA 40)	DLPFC (BA 9 BA 46)	Caud-ate
Barch et al. (1997)	Left			Left	Left	
Braver et al. (1997)	Left Right	Left	Left	Left Right	Left Right	Right
Cohen et al. (1997)	Left Right	Left Right		Left Right	Right	
Rypma et al. (1999)	Left Right	Left Right		Left		Left Right

The proposed design used in this study attempted to replicate the findings of Rypma et al. 1999 [6] and Barch et al. 1997 [7] while examining the effect of one working memory subcomponent in the context of another. To achieve this goal a factorial design with two factors, memory load and rehearsal period was used. Friston et al. [9] provide an example showing the benefit of a factorial design for investigating the importance of interaction among processes in cognition. In their paper, they describe the modulation of object recognition by phonological retrieval. Comparisons of tasks involving object recognition and those not involving object recognition revealed blood oxygen level dependent, BOLD, effects. However, it was not until the interaction of object recognition and phonological retrieval was tested that other modulating effects were revealed. The interaction term showed those regions that respond to object recognition only when phonological retrieval is also involved. This is why these "new" regions did not show effects in the initial comparisons.

The aim of this study was to reveal responses in the neural substrates described by Smith et al. as being involved in Baddeley's model of working memory using a factorial

design. Expected findings include DLPFC (BA 9/46), inferior frontal gyri (BA 44), inferior and superior aspects of the prefrontal gyri (BA 6), and posterior parietal regions (BA 7/40). The use of a two-factor design was not only to replicate the findings of others but also to investigate the relationship between the two working memory subcomponents. This study questioned whether there may be some interaction between the two factors of the experiment. The study was designed to test this question about the involvement of regions that increase in activity when the memory load and rehearsal period are varied. Responsiveness of regions during the interaction test provides evidence that activation in the region is evoked when the two factors interact. This interaction is not testable in designs that vary demands on each slave subcomponent independently.

2.2 Functional Magnetic Resonance Imaging Background

The signal measured in magnetic resonance imaging (MRI) comes from the protons of water molecules. When a subject is placed in a large magnetic field, some of their tissues' water molecule protons align their magnetic moments with the external field. The number of protons aligned with the external field is related to the external magnetic field strength. The MRI unit used in this experiment had a field strength of 1.5 Tesla, which is 37,500 times stronger than earth's average field strength of $4*10^{-5}$ Tesla. To create a signal, an excitation radiofrequency magnetic field pulse (rf pulse) is applied to the area of interest, for this experiment only the brain is of interest. The alignment of the protons absorbing this pulse changes to that of the rf pulse. After the short rf pulse, the protons begin to realign themselves with the external field and induce a signal voltage detectable with an external antenna.

The length of time required for a proton to realign itself with the external field is related to its surrounding tissue. Each tissue type has its own relaxation time constant called its T1 relaxation time. For the brain, there are three tissue types of interest, gray matter, white matter and cerebrospinal fluid (CSF). CSF has the longest T1 relaxation time and white matter has the shortest with gray matter's T1 relaxation time being closer to that of white matter than CSF. An image whose signal intensity relies on this T1 relaxation time is called a T1 weighted image. [10]

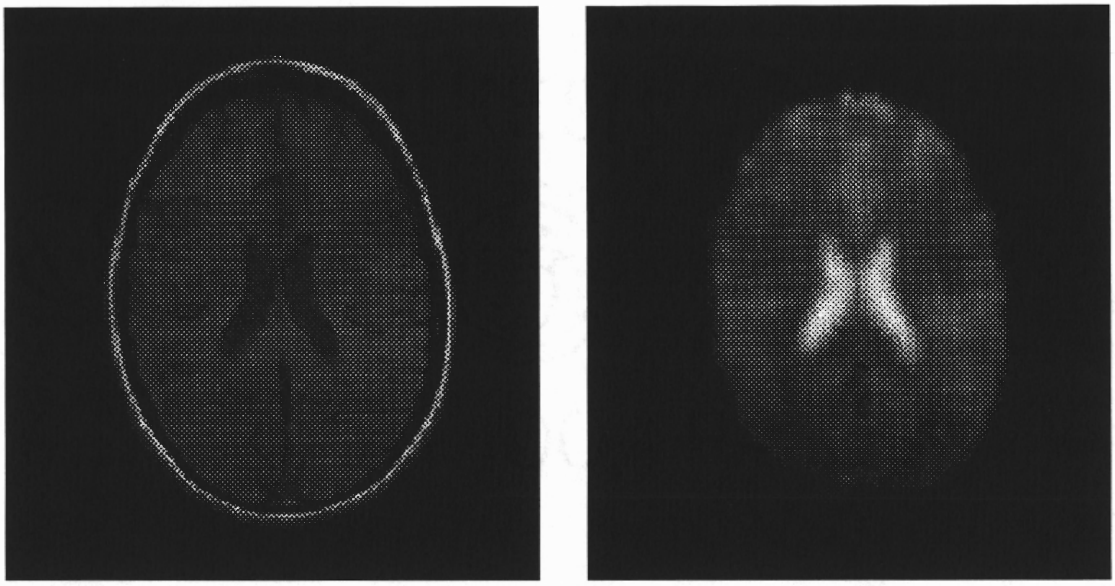

Figure 2.1 Left: T1 weighted MR image with cervical spinal fluid appearing black. Right: T2* weighted image with cervical spinal fluid appearing white.

Seen in the left hand side of Figure 2.1 is a T1 weighted image. Not including the scalp, the tissue with the greatest signal intensity is the white matter with the gray matter being slightly darker and the CSF in the ventricles being the darkest. The reason for these intensity differences is due to T1 relaxation time differences. Creating an image that has differential signal intensities for the different tissue types requires reading the signal strengths before the different tissues completely relax. Figure 2.2 shows relative T1 relaxation time courses for the three tissue types. By acquiring an image at the readout time indicated in the figure, the different tissue types will have different intensity values.

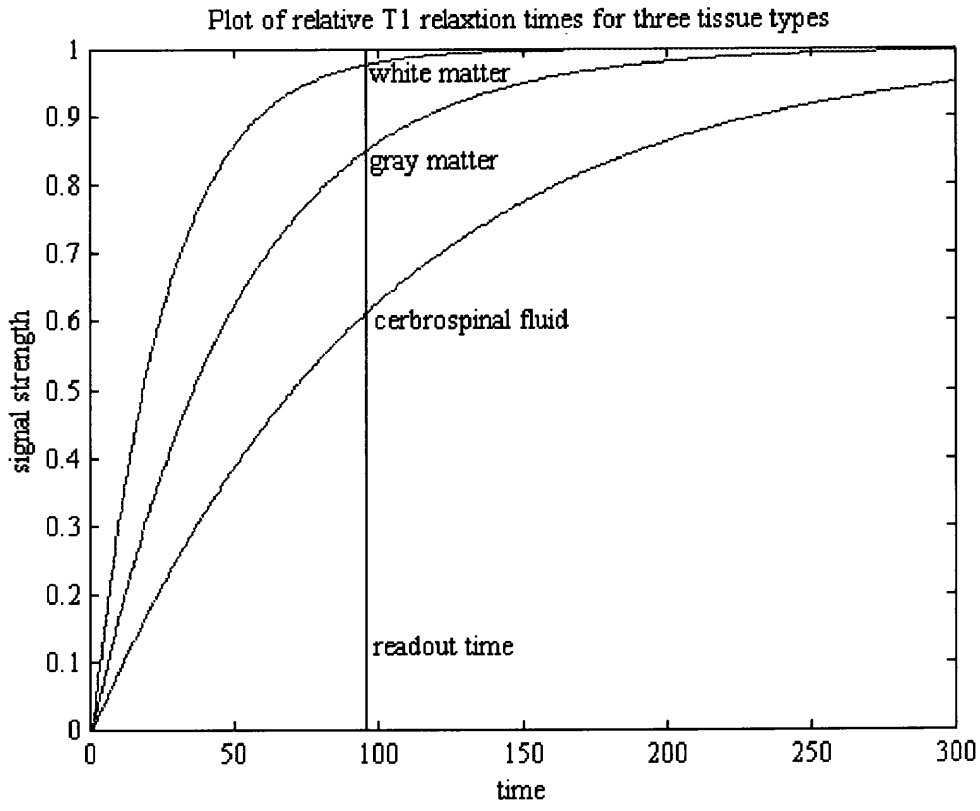

Figure 2.2 T1 Relative Relaxation Curves

T1 relaxation is not the only relaxation time occurring while protons realign themselves with the external field. A proton that is aligned with a magnetic field precesses, or spins, about the direction of the field as seen if Figure 2.3. After the rf pulse, the protons are in line with the rf pulse and are still precessing about the external field direction. An ideal situation would be one where all the protons precess about the field axis at the same frequency. However, due to small differences in the local magnetic field the protons precess at slightly different frequencies. As the differences in protons' precessions increase over time, the signal intensity decreases due to destructive interference. This decrease in signal intensity has its own time constant called T2 relaxation time. As with the T1 relaxation time, different tissue types have different T2 relaxation times.

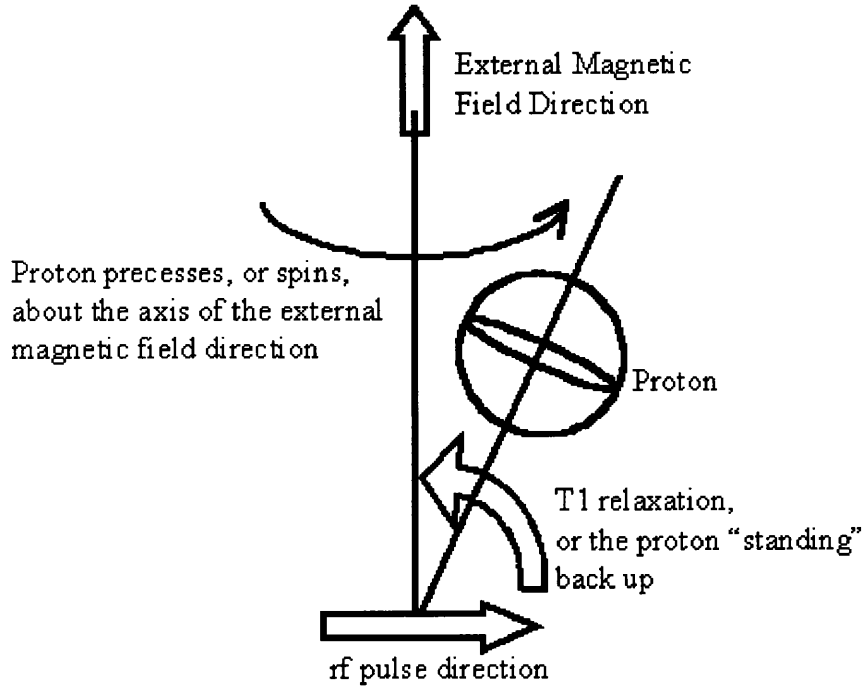

Figure 2.3 A proton precessing about an external magnetic field.

A further decrease in a tissue's T2 relaxation time is the presence of paramagnetic particles. The presence of a paramagnetic particle causes a more rapid decrease in T2 relaxation time and is referred to as T2' relaxation time. The sum of the T2 and T2' relaxation times is called T2* relaxation. A naturally occurring paramagnetic particle in the body is deoxyhemoglobin and its presence causes local T2* relaxation time to decrease and thereby reduce signal intensity more rapidly. An image relying on the T2* relaxation time is called a T2* weighted image.

Seen on the right hand of Figure 2.1 is a T2* weighted image. The tissue with the greatest signal intensity is the CSF with gray matter being slightly darker and white matter being the darkest. By reading the signal at the readout time indicated in Figure 2.4 a T2* image is created with the three tissue types being differentiable. Figure 2.4 shows relative T2* relaxation time courses for the three tissue types.

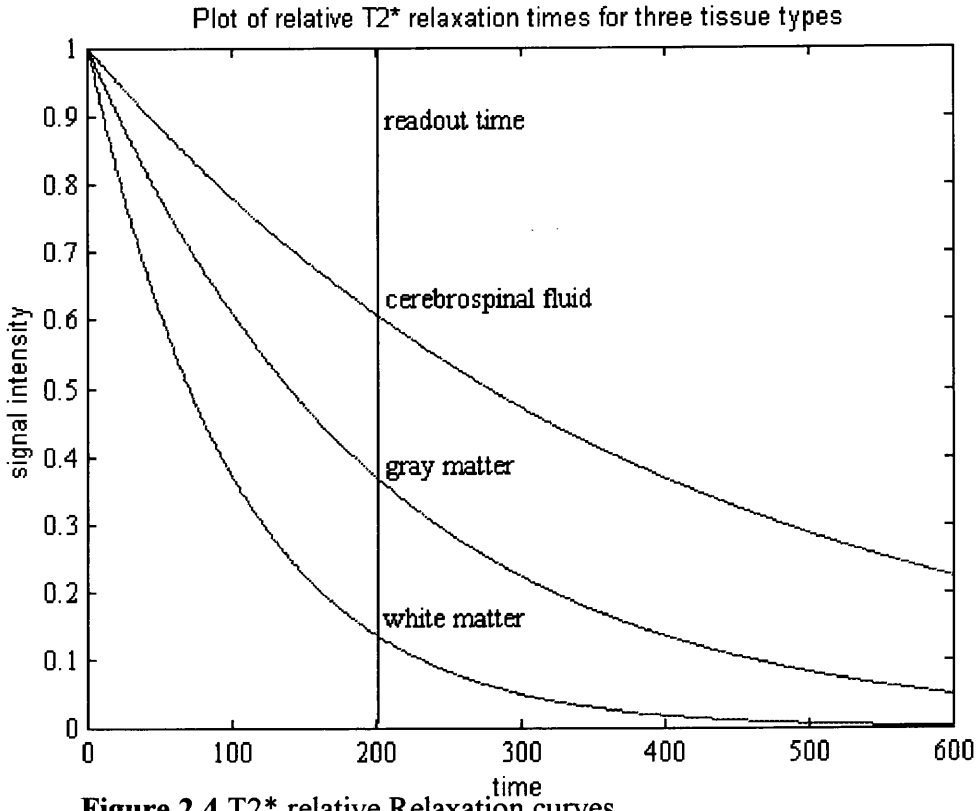

Figure 2.4 T2* relative Relaxation curves

Kwong et al. and Ogawa et al. [11, 12] used the natural presence of deoxyhemoglobin as a contrast agent to create the blood oxygen level dependent (BOLD) technique. The presence of deoxyhemoglobin in the blood causes a local decrease in signal intensity when acquiring a T2* weighted image, on the other hand a decrease in the local amount of deoxyhemoglobin will cause a local signal increase.

The presence of deoxyhemoglobin in blood vessels decreases when replaced by oxyhemoglobin thereby increasing the signal. When neuronal activation increases in a region, the body responds with an increase in oxygenated blood sent to the area. The amount of oxygenated blood sent to the area exceeds the needs of the tissues and the excess oxygenated blood drains into the venous system displacing the deoxygenated

blood and its deoxyhemoglobin. This displacement of deoxyhemoglobin causes a local signal change dependent on neuronal firing.

The rapid acquisition of T2* weighted images allows for the collection of images where the signal intensities change as a function of neuronal response. To get a rapid acquisition of images comes a trade off between spatial resolution and temporal resolution. To increase the temporal resolution of a time series, spatial resolution is sacrificed. In order to gain the temporal resolution of one scan every four seconds for this experiment images were acquired with the dimensions 64x64x28. The result is an image with voxel dimensions of 3.75mm x 3.75mm x 5mm (x, y, z).

With one image of the brain acquired every four seconds, for this experiment, changes in blood flow that occurred because of the task were detectable. The subjects engaged in the tasks and the neuronal responses increased the local blood flow resulting in detectable signal changes. After subjecting the images to spatial processing and statistical analysis, regional changes in blood flow to the brain that occurred as a result of engaging in the experimental task were detected.

CHAPTER 3

METHODS

3.1 Participants

All subjects signed an informed consent approved by the Institutional Review Board of the University of Medicine and Dentistry of New Jersey. Eight subjects (6 female, 2 male) between the ages of 21 and 43 (mean age of 32.5 years) participated in this study.

3.2 Task

The task used in this study consisted of two factors: memory load (i.e., number of items to be retained in the temporary storage buffer) and rehearsal period (i.e., length of time during which the items in the temporary storage buffer have to be rehearsed so the memory trace is maintained). Each factor had two levels. The memory load levels are two letters (Low) or five letters (High) and the rehearsal period levels are four seconds (Short) or twelve seconds (Long).

A graphical example of this is seen in Figure 3.1. This figure shows the two factors of this experiment, memory load and delay, each with their two levels. The result is four conditions, or as shown here the four cells of the experiment.

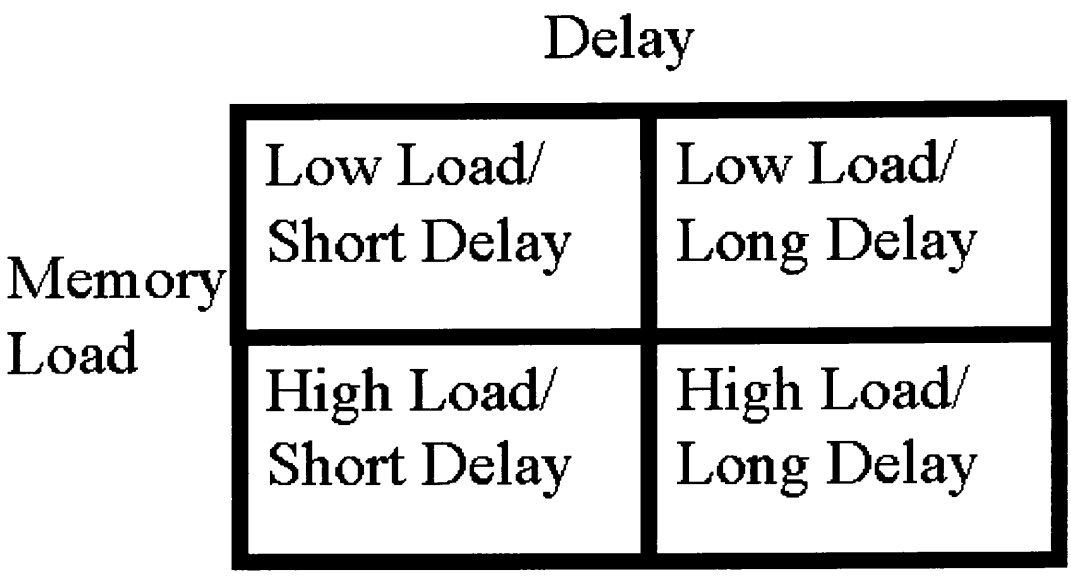

Figure 3.1 The experiments' two factors each with their respective two levels

With a two-factor design two main effects exist, one for each factor, and an interaction term. Testing of the memory load main effect involved a contrast consisting of subtracting the two low load conditions from the two high load conditions {(High/Long + High/Short) – (Low/Long + Low/Short)}. The main effect of memory load is designed to show those brain regions selectively associated with an increase in memory load.

Testing of the rehearsal period main effect involved a contrast consisting of subtraction of the two short rehearsal period conditions from the two long rehearsal period conditions {(High/Long + Low/Long) – (High/Short + Low/Short)}. The main effect of rehearsal period is designed to reveal those brain regions selectively associated with an increase in the length of rehearsal period.

What this experiment has to offer beyond the testing of two main effects is the test of an interaction between the two factors. The interaction tests for those brain regions selectively more sensitive to the difference between high memory loads in long versus short rehearsal periods than low memory loads in long versus short rehearsal periods

{(High/Long - High/Short) - (Low/Long - Low/Short)} [13]. This test therefore reveals brain regions more selective for the high memory load and long rehearsal period conditions. The converse of this test is that which tests for those regions selectively more sensitive to the difference between low memory loads in long versus short rehearsal periods than high memory load conditions in long versus short rehearsal periods {(High/Short – Low/Short) – (High/Long – Low/Long)}. This test reveals brain regions more selective for the high memory load and short rehearsal period conditions.

To summarize these contrasts see Table 1. The columns represent the four conditions of the experiment and the rows represent the four different tests. Take row one as an example. The test is the Main Effect of Rehearsal Period, and the contrast vector is (-1 -1 +1 +1). This test multiplies the respective columns by the value in each box, either -1 or +1. The result is –{Low Load / Short Delay} – {High Load / Short Delay} + {Low Load / Long Delay} + {High Load / Long Delay}.

Table 2 Summary of test performed and their contrast vectors

Test	Low Load / Short Delay	High Load / Short Delay	Low Load / Long Delay	High Load / Long Delay
Main Effect of Rehearsal Period	-1	-1	+1	+1
Main Effect of Memory Load	-1	+1	-1	+1
Test for sensitivity of a High Load held over a Long Delay	+1	-1	-1	+1
Test for sensitivity of a High Load held over a Short Delay	-1	+1	+1	-1

3.3 Experimental Procedure

The task included thirty-two trials with each trial lasting twenty-four seconds. Within the first five seconds of each trial, the letters of the memory load were presented. Following was the delay period and finally a probe letter presentation. Within a low load memory level and short rehearsal period trial, two letters were presented in the first five seconds followed by a four second delay and finally probe letter presentation. The inter-stimulus time interval for a trial with a short delay is thus thirteen seconds. A high load memory level with a long rehearsal period consists of five letters presented in the first five seconds of the task followed by a twelve second delay period and concluding with the probe letter presentation. For a long delay period block the inter-stimulus time interval is five seconds.

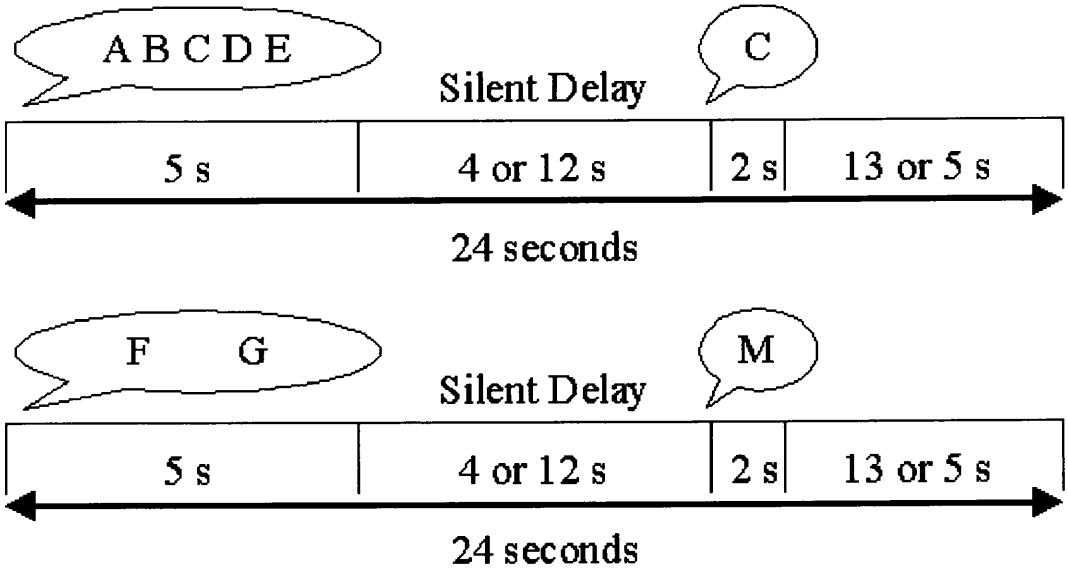

Figure 3.2 The Behavioral Experiment

Figure 3.2 shows a graphical representation of the task. The top row shows the presentation of five letters with the bottom showing two letters.

3.4 fMRI Scanning

A 1.5 Tesla GE Signa scanner was used to acquire all data for this study. Prior to functional scanning T1 anatomical images were obtained for data overlay. (256x256x28 voxels, Field of View = 240x240 mm, slice thickness=5 mm) Functional images consisted of 28 slice T2* weighted echoplaner images chosen to cover the entire brain. (TR/TE=4000/60 ms, 64x64x28 voxels, Field of View=240x240 mm, slice thickness=5mm) Functional data were acquired during one session lasting 13 minutes. A total of 195 images were collected with the first three discarded to allow for T1 equilibrium effects. Subjects were reminded not to move and their heads were restrained with padding.

3.5 Data Analysis

3.5.1 Spatial Processing

All data were analyzed using Statistical Parametric Mapping software (SPM99 Wellcome Department of Cognitive Neurology, London, UK) [14]. A first step in the analysis of the time series data is to set the origin of all the images. The origin of the images is the reference point from which locations are measured in Euclidean space, in millimeters. As a default, the origin field of the images is set to the center of the data volume. Before the experiment was carried out, the decision was made to transform all of the data into a standard space. Transforming all data into a standard space allows for cross subject comparisons and therefore group analysis. The standard space chosen was that designed by Talairach and Tournoux [15]. The origin of their standard space was chosen to be an anatomical landmark called the Anterior Commisure and therefore the origin of all

images was set to this same anatomical location. From this location, distances in millimeters are measured. Each time point in the time series is stored as a separate image file. Accompanying every image file is a header file, which has a description of the data file. One descriptor is which voxel in the image file is the origin. By editing the header file one changes the origin.

The next step is to realign the entire time series data. Even though the subjects were instructed not to move their head and cushions were in place to restrict head motion, movement of the head still occurs. To realign the time series, the brain was considered a rigid body. This means that six parameters are necessary to transform one rigid body into the space of another. The six parameters are x, y, z translations and roll, pitch, yaw rotations.

Aligning two images requires the images to be adjusted until their sum of squared differences is minimized. The sum of squared difference of two images is the subtraction of the two images from each other and the square of the resultant image. When the image alignment is as close as possible, the resultant image will be at its minimum. The determination of the realignment parameters is performed in an iterative fashion and stopped when the sum of squared difference stops decreasing. The results of this iterative optimization are three four by four matrices. These matrices describe the necessary translations and rotations to transform one image into the space of another. Figure 3.3 shows these matrices. [16]

$$\begin{pmatrix} 1 & 0 & 0 & x_{trans} \\ 0 & 1 & 0 & y_{trans} \\ 0 & 0 & 1 & z_{trans} \\ 0 & 0 & 0 & 1 \end{pmatrix} \begin{pmatrix} 1 & 0 & 0 & 0 \\ 0 & \cos(Q) & \sin(Q) & 0 \\ 0 & -\sin(Q) & \cos(Q) & 0 \\ 0 & 0 & 0 & 1 \end{pmatrix} \begin{pmatrix} \cos(F) & 0 & \sin(F) & 0 \\ 0 & 1 & 0 & 0 \\ -\sin(F) & 0 & \cos(F) & 0 \\ 0 & 0 & 0 & 1 \end{pmatrix} \begin{pmatrix} \cos(W) & \sin(W) & 0 & 0 \\ -\sin(W) & \cos(W) & 0 & 0 \\ 0 & 0 & 1 & 0 \\ 0 & 0 & 0 & 1 \end{pmatrix}$$

Figure 3.3 Q, F, and W in radians are the rotation angles about the X, Y, Z axes respectively

Application of the above matrices to a voxels' coordinates involved multiplying the matrices together in the order above and the resultant matrix was multiplied to the coordinates of the voxel (x_1, y_1, z_1, 1). The new set of coordinates (x_2, y_2, z_2, 1) were then in the transformed space.

One goal of the analysis was to allow comparisons between the results and the results from other research groups. In order to do this, the data was spatially normalized to Talairach coordinates [15]. Talairach and Tournoux created a human brain atlas that contains a coordinate system allowing locations to be described with a set of three-millimeter distances from the origin, the Anterior Commisure. It is this standard space that the data was transposed into for cross subject and experiment comparisons.

In order to do this normalization the functional data were first co-registered with the high-resolution anatomical image [17]. This registration was done between a mean functional image and the high-resolution image, the resultant translation and rotation matrix was than applied to all images of the time series placing all images into the same space as the high-resolution anatomical image. The reason for this registration is to account for any subject movement that may have occurred between the time of the anatomical scan and the beginning of the functional scanning. That time was approximately twenty-five minutes. This step also allows for accurate overlay of the functional results onto the same subject's high-resolution anatomical image.

Placing two images into the same space that are of different imaging modalities, such as T1 weighted and T2* weighted, requires a procedure different from that implemented in realigning images. First the T1 image was aligned to a T1 template image and then the T2* image was aligned to a T2* template image. Instead of the six-parameter estimation as used in the realignment step, 12 parameters are estimated at this step for both images. The extra six parameters are three shear and three zoom parameters. Figure 3.4 shows diagrams exemplifying these 12 parameters.

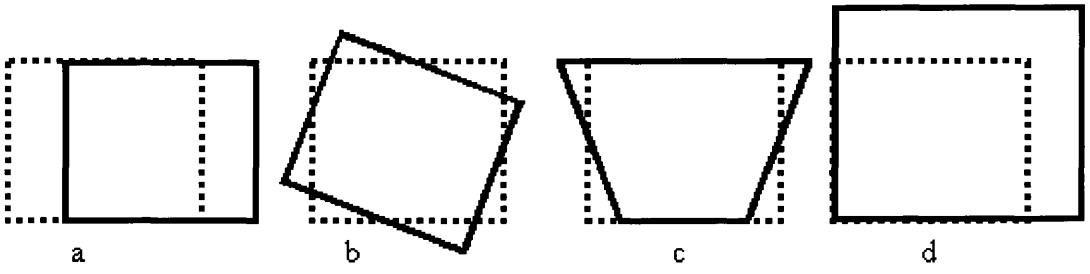

Figure 3.4 Examples of four types of transformation, a: Translation, b: Rotation, c: shear, d: zoom

After the two images are in the same space as the two template images, they were partitioned. Brain tissue comes in three main categories, gray matter, white matter, and CSF. Using template probability images of the three tissue categories, the two images were segmented into three images each. The use of template probability images makes a determination for each voxel in the images as to which category the voxel belongs to.

The resultant six images (T1 gray, white, CSF and T2* gray, white, CSF) were simultaneously registered together. A rigid body transformation was performed with the same optimization technique as used in the realignment stage. Using the transformation matrices for the T1 image to its template, the T2* image to its template and the segmented T2* images to the segmented T1 images the T2* mean image and the T1 anatomical images were transformed into the same space.

Another benefit of this registration appears in the spatial normalization step. This step uses a 12-parameter transformation and a non-linear approach to put an image into the standard Talairach and Tournoux space [16]. With the high resolution and functional images in register, the parameters necessary to spatially normalize the high-resolution image are applicable to the entire low-resolution functional time series. The larger amount of spatial information in the high-resolution image allowed for a more accurate set of transformation parameters to be obtained. The twelve parameters are three translational, three rotational, three zoom and three shear as seen above in the coregistration step and Figure 8. The determination of the twelve parameters was done with the same optimization technique as used in the realignment step; however, this time the T1 image was transformed into the space of a template image.

To account for local differences between the T1 anatomical image and the template image not accounted for by the affine transformations, non-linear deformations were performed. Sets of 3-D cosine functions were used as a basis set for the non-linear deformations. [18]

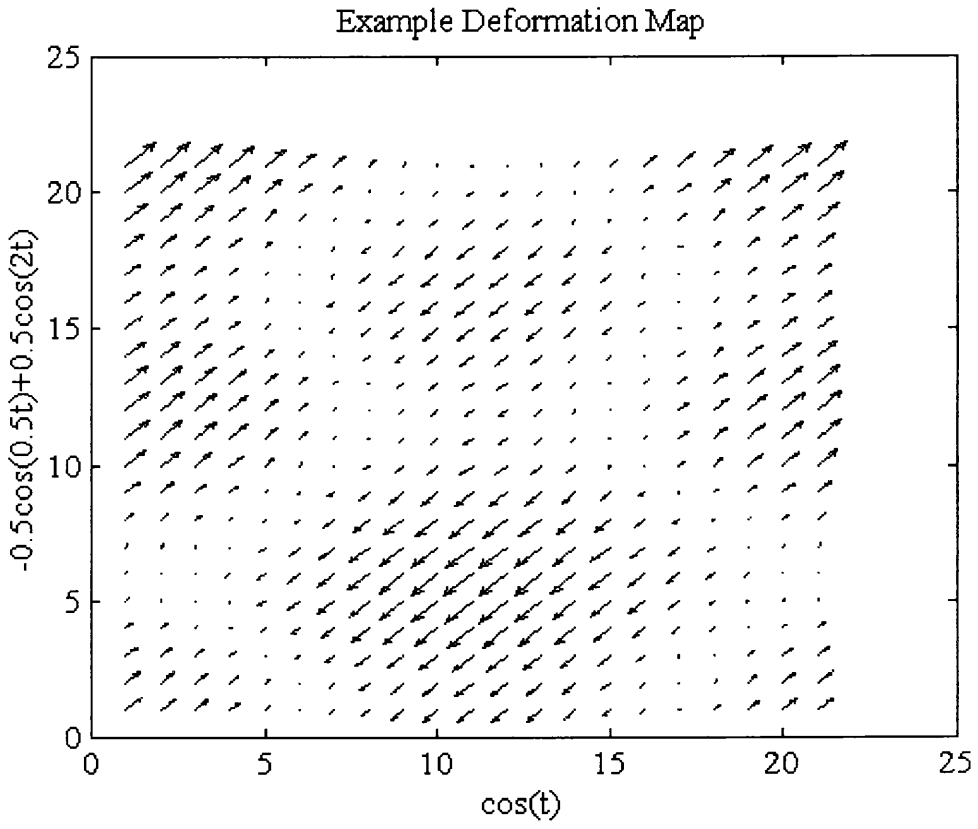

Figure 3.5 Example Deformation Field

Figure 3.5 best describes a deformation map made of cosine functions. The directions of the arrows indicate the direction of deformation while the lengths of the arrows indicate the amount of deformation. The axes in the above plot indicate the cosine functions used to generate this plot. This deformation map is made of a sum of cosine functions; therefore, it can account for any necessary deformations. This can be compared to Fourier Series where any function can reasonably be represented by the sum of a set of sine and cosine functions. This same technique is applied here in three dimensions. Due to memory limitations, only eight cosine functions in each direction were used to create this deformation map. Again, an iterative method was performed in order to minimize the sum of squared differences between the template image and the T1 anatomical image.

Following the determination of realignment, co-registration and normalization parameters the application of these parameters was performed. All estimated parameters were applied by sinc interpolating the images into their new space. The result was a new series of images all in the same standard space and in register with each other. Sinc interpolation uses a Hanning windowed sinc function. The Hanning window was applied so that only a 9x9x9 cube of voxels was used to determine the new value of a transformed voxel. The sinc interpolation was performed in each of the three directions separately. The Hanning windowed sinc function using nine nearest neighbors in one dimension is: $\sum_{i=1}^{9} v_i \frac{\frac{\sin(\pi d_i)}{\pi d_i}\frac{1}{2}(1+\cos(2\pi d_i / 9)}{\sum_{j=1}^{9}\frac{\sin(\pi d_i)}{\pi d_i}\frac{1}{2}(1+\cos(2\pi d_i))}$

Where d_i is the distance from the sampling point to the center of the ith voxel and v_i is the ith voxel's value. An example of a sinc function is seen in Figure 3.6.

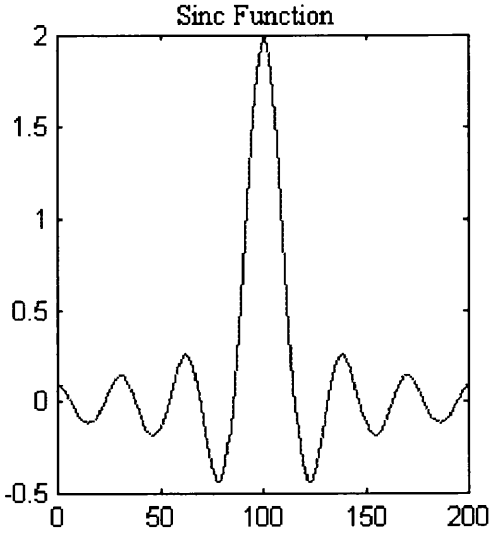

Figure 3.6 An example of a sinc function. $\frac{\sin(\pi t)}{\pi t}$

The final step in what are called the preprocessing steps is to smooth the data in three dimensions; this step suppresses noise in the data. Smoothing the data involved the convolution of every voxel with a Gaussian curve in each of the three directions, x, y, z.

The new value of a voxel was: $t_i = \sum_{j=-d}^{d} s_{(i-j)} g_i$

Where $s = \frac{FWHM}{\sqrt{8\ln(2)}}$ and $g_j = \frac{e^{-\frac{j^2}{2\pi s^2}}}{\sqrt{2s^2}}$ and seen if Figure 3.7.

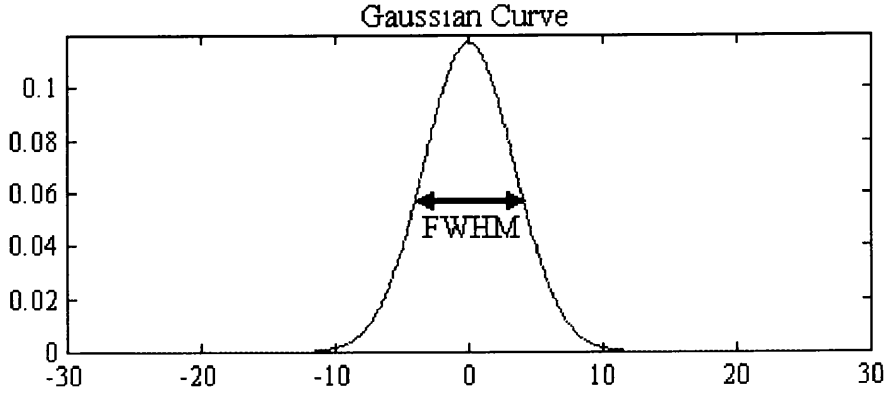

Figure 3.7 A Gaussian Curve

FWHM refers to the full width at half maximum as indicated in Figure 3.7. This parameter determines the amount of smoothing applied to the images. The FWHM applied to the functional data was 8 mm, 8 mm, 10 mm in the directions x, y, z respectively.

Before the statistical analysis, the data was temporally band-pass filtered. The low frequency cutoff was 192 seconds and the high pass cut off for the filter was the hemodynamic response. The hemodynamic response is the waveform of the blood flow as it responds to an increase in neuronal activation. The hemodynamic response function

[19] is modeled as the difference between two Gamma functions and is intended to provide a canonical model of the hemodynamic of the brain. The aim of using this information is to improve the statistical analysis by incorporating physiological information into the statistical model. The hemodynamic response function takes into account the delay and dispersion of the blood flow response to neural activation. Since this information is used in the model, the data is filtered at this high frequency response to exclude any variations that occur above it.

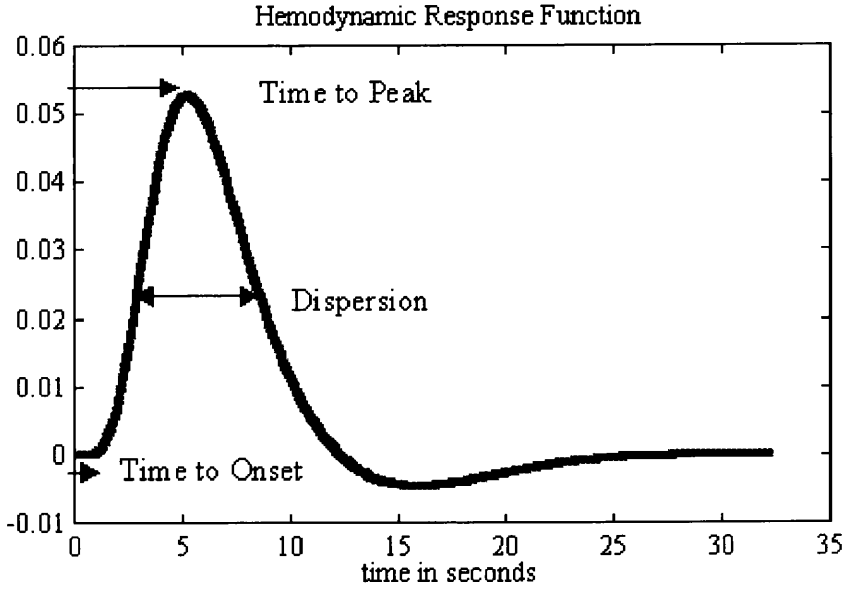

Figure 3.8 The hemodynamic response function

Figure 3.8 shows the hemodynamic response function and three of its properties the time to onset (when the blood flow begins to rise), the dispersion, and the time to peak (how long before the blood flow reaches its maximum value).

The next step was global intensity normalization of the data. Global intensity normalization scales the data to have a mean of 100. To scale the data, first, the mean value of each image was subtracted from each voxel in the image and then 100 were added to the each voxel. The mean value of each image is now 100. With the mean of the

images scaled to one hundred the parameter estimates resulting from the least squares analysis are also interpretable as percent signal changes. Percent signal changes hold more meaning in the context of detecting signal changes with functional MR imaging than do parameter estimates of a response. The number is the same but the interpretation is more meaningful when referred to as a percentage.

3.5.2 Statistical Analysis

The assessment of a significant relationship of a voxel in the fMRI time-series data and the behavioral experiment is based on multiple linear regression. The first step in statistical analysis of this form is the creation of a design matrix. Figure 3.9 shows the design matrix used in this experiment. This design matrix incorporates all of the behavioral task conditions and timing parameters. The design consists of four conditions, one condition per cell of the factorial design. This corresponds to one condition in the design for each of the following: low memory load and short rehearsal period, high memory load and short rehearsal period, low memory load and long rehearsal period, and high memory load and long rehearsal period. The columns of the design matrix represent each of these conditions of the experiment and the rows of the design matrix represent the time points of the experiment. A fifth column is included in this design matrix, which only consists of the number one. This column of ones corresponds to the y-intercept of the linear regression as well as the overall mean.

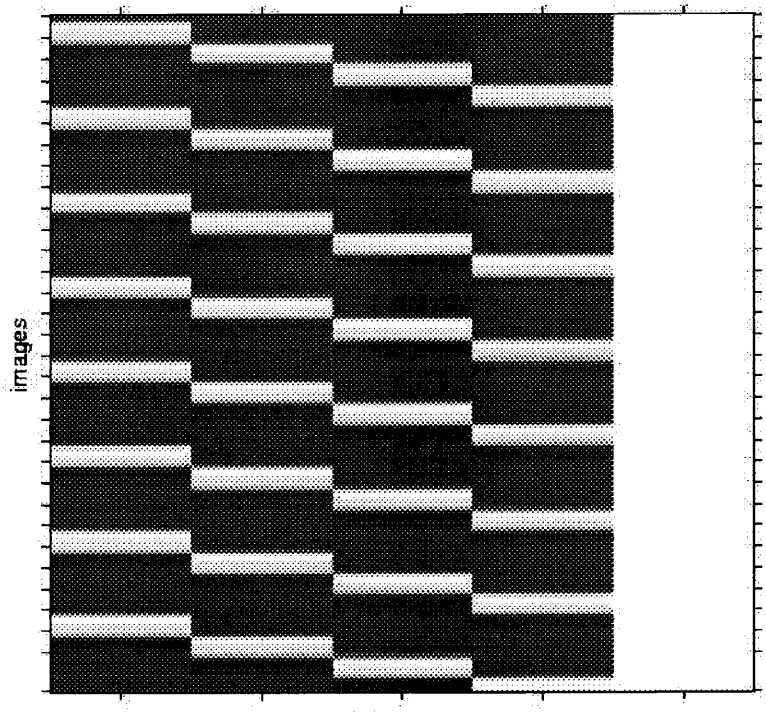

Figure 3.9 The design matrix used in the experiment

To incorporate the information describing the behavioral conditions of the experiment each of the designs' columns consisted initially of ones and zeros. A one in a column means that during this time-point the subject was engaged in the behavioral condition described by this column and a zero means that the subject was not engaged in this condition. Convolution of the above described hemodynamic response function and the columns of the design matrix incorporate physiological information into the model with the intent of increasing statistical power. After this convolution, the columns of the design matrix no longer consist of zeros and ones but values with a range around zero. The columns now represent the "engaged or not-engaged" blocks convolved with the hemodynamic response function.

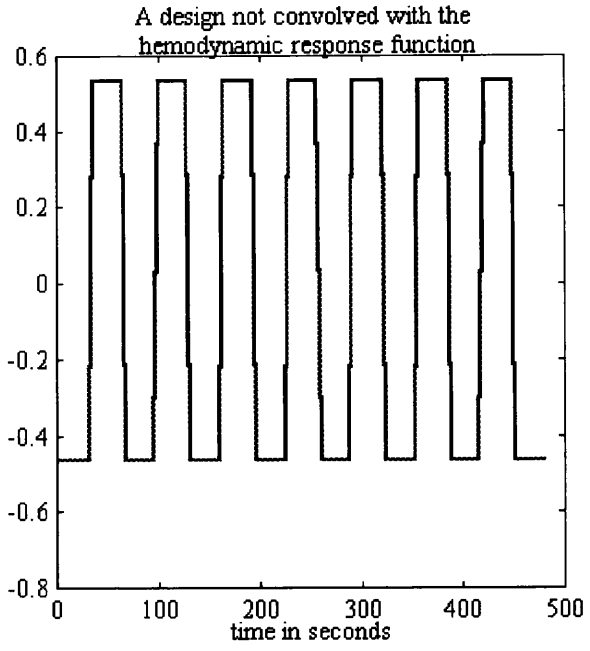

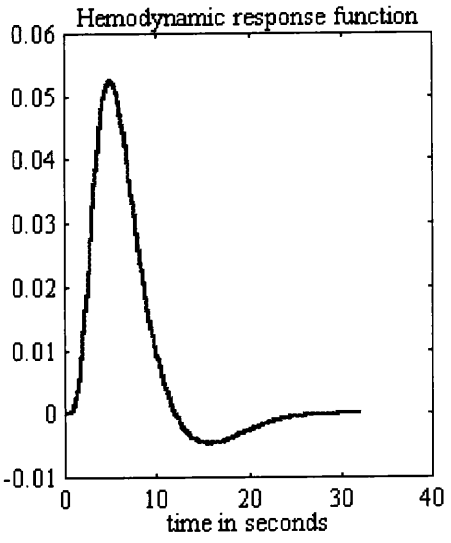

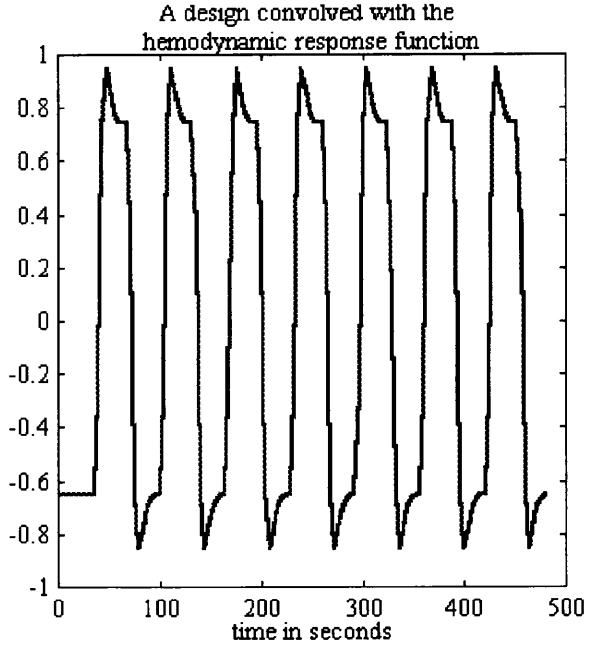

Figure 3.10 An example design before and after convolution with the hemodynamic response function.

Figure 3.10 shows the plot of an example design. The upper left hand plot shows the design consisting of two levels. The upper right hand plot shows the hemodynamic response function and the lower plot shows the two plots convolved together. The lower plot is a better fitting model than the upper left hand plot due to its incorporation with the hemodynamic response function.

The result of the least squares estimation of parameters for the data and model are referred to as beta weights in this context, and are also known as regression slopes. For each voxel and each column of the design matrix there is a beta weight estimated by the least squares estimation. The result is therefore five "beta images," one for each column of the design matrix. The beta weight for one voxel and one column of the design matrix represents the relationship between the time course of the data and the time course of the behavioral condition. An increase in a beta weight value represents an increase in the relationship between the time course of that behavioral condition and that voxel's time course. To perform the tests as described above, the main effects and the interactions, are tested with linear combinations of these beta-images, called contrasts. The contrasts used in the experiment are described above in Section 3.2 and displayed in Table 1.

The result of performing one of the above tests is a statistical parametric map. The described contrasts were tested with t-tests; therefore, the resultant statistical parametric map is a t-map. Determination of significance of a voxel was performed with thresholds placed on the t-map. Two thresholds were placed on the t-maps, a height threshold and an extent threshold. Figure 3.11 displays these two thresholding techniques. If the height threshold is set at threshold 1 and the extent threshold is set to zero, only clusters e and f containing peaks B and C would be revealed. An extent threshold of zero means that

clusters of any size activated above the height threshold are revealed. At height threshold 2, with an extent threshold of zero peaks B and C are one large cluster g and cluster h containing peak D is also revealed. If the height threshold is placed at threshold 2 and the extent threshold is implemented then only the large cluster g of peaks B and C is revealed. The extent threshold eliminates the small peak D because its extent of h is less than the threshold.

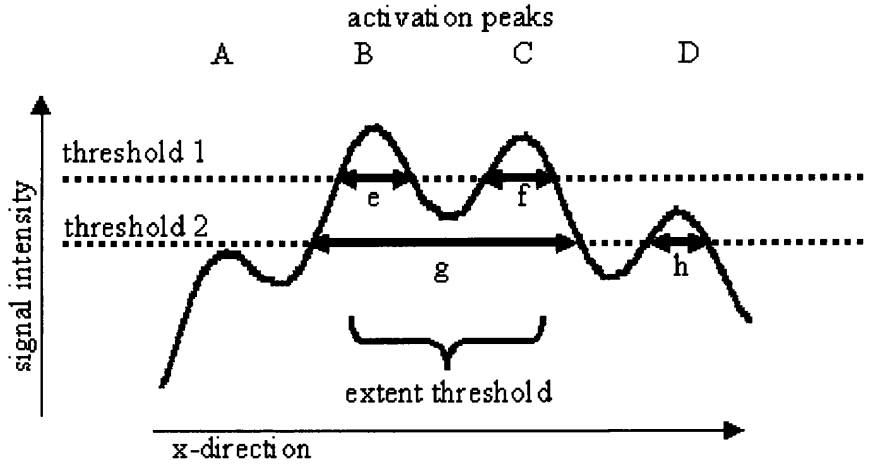

Figure 3.11 Example of height and extent thresholds.

3.5.3 Group Analysis

The overall aim of this study is to have the ability to make inferences about the population from which the subjects were drawn [20]. A first step in the group analysis of the data is to only include voxels that are included in each subject's time-series data. Due to the variability in signal dropout across subjects [23], only the minimum of all brains is included for analysis. In the analysis, this is interpreted as that the subject with the greatest amount of signal drop out places the largest limitation on the group results. The group level statistics are performed only on those voxels included in every subject in the

group. If a voxel has data for all but one subject in the group, than this voxel is not included in the final group analysis.

To make population inferences, each subject is treated as a random, independent variable. In order to do this two types of variation are in need of consideration. First, is the inter-scan within subject variance and the second is the between subject variance. At the first step of this statistical analysis, each subject is tested individually. This accounts for the inter-scan variability. A contrast image of each test of interest and each subject is then taken to a second step for the group analysis. The contrast image from each subject is an image where each voxel is a linear combination of beta weights. The second step of this analysis performs a one-sample t-test on this series of contrast images. This tests for voxels that show a significant difference from zero. The voxels showing significant differences from zero correspond to areas selectively responsive to the test after intra and inter subject variance is accounted for. This means that statistical significance of a voxel after this stage of analysis is generalized to the population.

Anatomical substrates of clusters of significant pixels were assessed using the Talairach Daemon (RIC, UTHSA) [21]. The Talairach Daemon is an online database of the Talairach and Tournoux Atlas. Submitting a set of x, y, z coordinates (in millimeters) to the database results in finding the hemisphere, tissue type and region of the voxel in the brain. All voxels showing significance in relation to a contrast were examined. Within the software used for the analysis of the data, a cluster's location is defined by its maximum. The problem with this approach is the fact that clusters have great variability in size. For a small cluster, knowing just the location of the cluster maximum may be enough information to describe the location of that cluster. However, large clusters can

extend over neighboring brain regions and the location of this clusters' maxima may not accurately describe it. For example, a cluster has a size of 400 contiguous voxels and the local maxima describe the location of this cluster as being in Brodmann's area 44. Does this mean that 400 contiguous voxels are significant in Brodmann's area 44? Or should this be interpreted as Brodmann's area 44 is activated along with its neighbors, BA 45, 9 and 6? Inspection of just the local maxima within a statistical parametric map does not shed light on this question. Even within one Brodmann's area that extends over more than one gyrus or different aspects of the same, one may require more information than the cluster's maximum to describe its extent.

Another situation is a cluster on the brain's midline. The cluster may have an extent of four hundred contiguous voxels with its maximum located in the right hemisphere. Does this mean that this entire cluster exists in the right hemisphere? Inspection of the brain map could tell you otherwise; however, the amount of significant voxels in each hemisphere is still unknown.

To circumvent the above difficulties, all significant voxels were investigated within a statistical map instead of just the locations of the maxima. The result is a large table of voxel coordinates, one set for every activated voxel in the brain map. The Talairach coordinates for each voxel are determined with the Talairach Daemon (RIC, UTHSCSA) and the result is the Talairach location for every single significant voxel. This data file is sorted by the different neural substrates; and the number of significant voxels per different neural substrate determined. This table of summary information of a statistical map allows one to address the questions posed above. If a cluster extends over multiple regions one now knows the exact extent of the cluster.

Appendixes A, B and C contain programs written in Matlab used to perform the above steps. The program jrsstreamTAL.m in Appendix A extracts the x, y, z coordinates from the SPM99 software and saves them to a file. The program roital.m summarizes the results of the Talairach Daemon and creates a table showing the number of activated voxels in each different region of the brain. The program saves this table to a file. Appendix C has the program called merge.m, which merges two tables from roital.m and allows for the comparison of two results.

CHAPTER 4

RESULTS

4.1 The Main Effect of Rehearsal Period

Contrasting all conditions involving a long rehearsal period with all tasks involving a short rehearsal period will reveal brain regions selectively associated with an increase in the length of rehearsal period [13]. This test revealed activation in bilateral medial frontal gyri (BA 9 and 6), bilateral superior frontal gyri (BA 6 and 44), left inferior parietal lobule (BA 40) and bilateral cingulate gyri (BA 32).

The entire sub-vocal rehearsal circuit was active in this task as well as the pure storage buffer. The DLPFC that is hypothesized to perform executive functions is also active within this task. These results are summarized in the first column of Table 3 and seen in Figures 4.1.

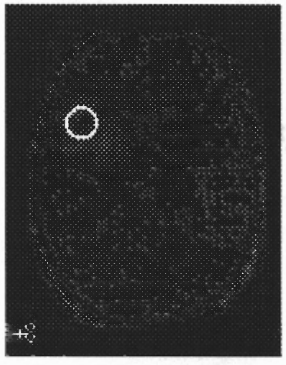

Inferior Frontal Gyrus

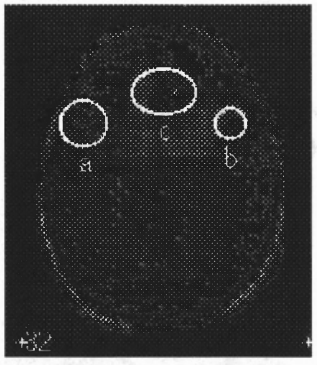

a, b: Bilateral Medial Frontal Gyrus, c: Cingulate Gyrus

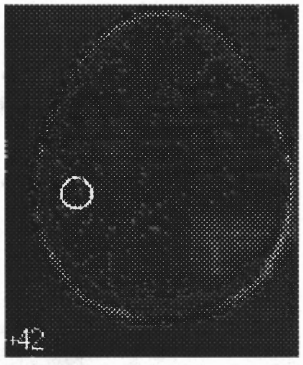

Inferior Parietal Lobule

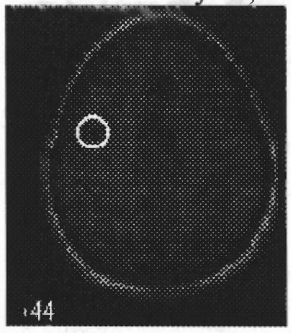

Medial Frontal Gyrus

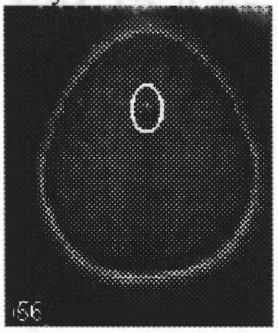

Superior Frontal Gyrus

Figure 4.1 Activity during the main effect of rehearsal period

Table 1
Results for all tests

Hemisphere	Lobe	Region	Brodmann Area	Main Effect of Rehearsal Period	Main Effect of Memory Load	Interaction High Load over Long Delay	Interaction High Load over Short Delay
Left Cerebrum	Frontal Lobe	Inferior Frontal Gyrus	9	2			
Right Cerebrum	Frontal Lobe	Inferior Frontal Gyrus	9	1			13
Left Cerebrum	Frontal Lobe	Medial Frontal Gyrus	9	7			
Right Cerebrum	Frontal Lobe	Medial Frontal Gyrus	9	48			
Right Cerebrum	Parietal Lobe	Paracentral Lobule	7			2	
Right Cerebrum	Parietal Lobe	Precuneus	7			28	
Left Cerebrum	Frontal Lobe	Medial Frontal Gyrus	6	25	11		
Right Cerebrum	Frontal Lobe	Medial Frontal Gyrus	6	48	9	19	
Left Cerebrum	Frontal Lobe	Middle Frontal Gyrus	6		11		
Right Cerebrum	Frontal Lobe	Middle Frontal Gyrus	6				9
Left Cerebrum	Frontal Lobe	Precentral Gyrus	6		12	13	
Right Cerebrum	Frontal Lobe	Precentral Gyrus	6			2	21
Left Cerebrum	Frontal Lobe	Superior Frontal Gyrus	6	26	19		
Right Cerebrum	Frontal Lobe	Superior Frontal Gyrus	6	62	51	1	2
Left Cerebrum	Frontal Lobe	Precentral Gyrus	44	4	5		
Right Cerebrum	Frontal Lobe	Precentral Gyrus	44	5			
Left Cerebrum	Parietal Lobe	Inferior Parietal Lobule	40	9			
Right Cerebrum	Parietal Lobe	Inferior Parietal Lobule	40				2
Right Cerebrum	Limbic Lobe	Anterior Cingulate	32	15			
Left Cerebrum	Limbic Lobe	Cingulate Gyrus	32	35	6		
Right Cerebrum	Limbic Lobe	Cingulate Gyrus	32	40	12		
Left Cerebrum	Frontal Lobe	Cingulate Gyrus	32	1			
Right Cerebrum	Frontal Lobe	Cingulate Gyrus	32	5			
Left Cerebrum	Sub-lobar	Caudate	Caudate Body		4		25
Right Cerebrum	Sub-lobar	Caudate	Caudate Body		3		15
Left Cerebellum	Anterior Lobe	Culmen	*		27		
Right Cerebellum	Anterior Lobe	Culmen	*		63		
Left Cerebellum	Posterior Lobe	Declive	*		302		
Right Cerebellum	Posterior Lobe	Declive	*		209		
Left Cerebrum	Sub-lobar	Thalamus	Ventral Lat. Nucl.			27	
Right Cerebrum	Sub-lobar	Thalamus	Ventral Lat. Nucl.			46	

4.2 The Main Effect of Memory Load

Contrasting all conditions involving a high memory load with all tasks involving a low memory load will reveal brain regions selectively associated with an increase of memory load. This test revealed activation in bilateral medial frontal gyri (BA 6), bilateral superior frontal gyri (BA 6), left middle frontal gyrus (BA 6), left precentral gyrus (BA 6), left inferior frontal gyrus (BA 44), bilateral cingulate gyri (BA 32), bilateral caudate body, left caudate head, bilateral thalamus, and bilateral culmen and declive of the cerebellum. This test also revealed activation in the rehearsal circuit but not the storage buffer. These results are summarized in the second column of Table 2 and seen in Figure 4.2.

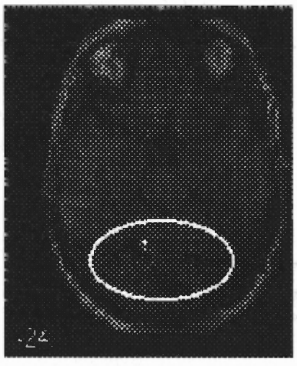

Cerebellum

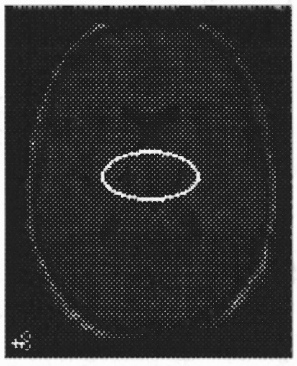

Thalamic Activity

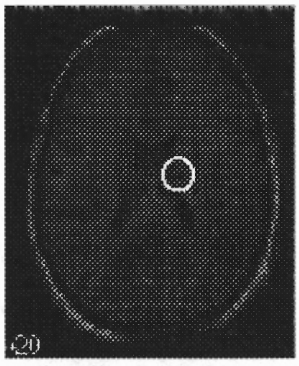

Caudate Activity

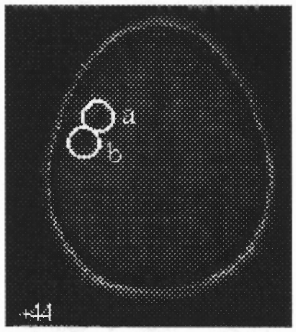

a: Middle Frontal Gyrus
b: Precentral Gyrus

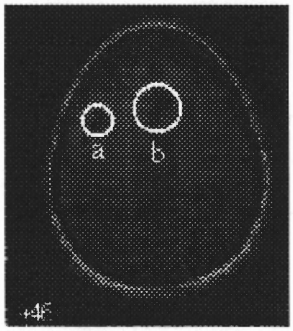

a: Medial Frontal Gyrus
b: Cingulate Gyrus

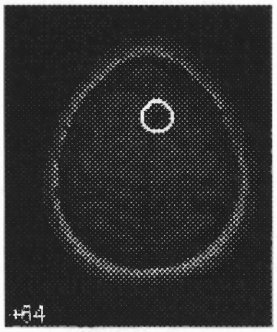

Superior Frontal Gyrus

Figure 4.2 Activity during the main effect of load

4.3 Interactions

4.3.1 Selectivity for High Load and Long Rehearsal Periods

This interaction test is designed to reveal brain regions selectively associated with a high memory load and a long rehearsal period while avoiding any confounds of the two main effects. This test revealed activation in right parietal regions (BA 7), right medial frontal gyrus (BA 6) and bilateral precentral gyri (BA 6). These results are summarized in the third column of Table 2 and seen in Figures 4.3.

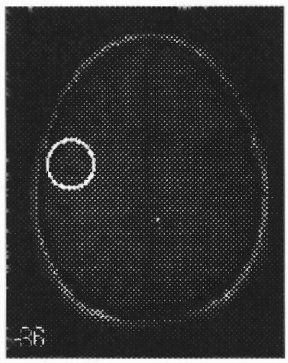
Precentral Gyrus

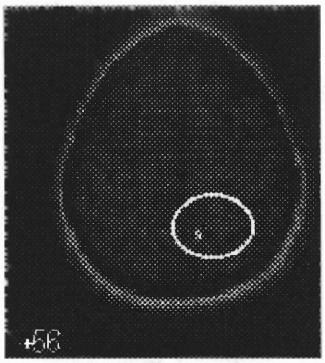
Parietal Cortex

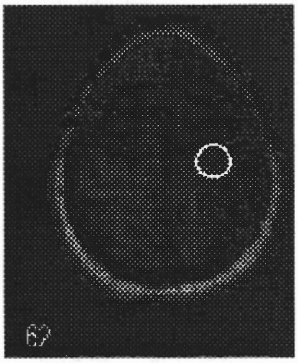
Medial Frontal Gyrus

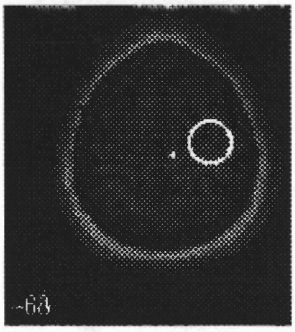
Precentral Gyrus

Figure 4.3 Activity during the test for sensitivity to a High Load held over a Long Rehearsal Period

4.3.2 Selectivity for High Load and Short Rehearsal Periods

This interaction test is designed to reveal brain regions selectively associated with a high memory load and a short rehearsal period while avoiding any confounds of the two main effects. This test revealed activation in right inferior frontal gyrus (BA 9), right middle frontal gyrus (BA 6), right precentral gyrus (BA 6), right parietal regions (BA 40), and bilateral caudate body. These results are summarized in the fourth column of Table 2 and seen in Figure 4.4.

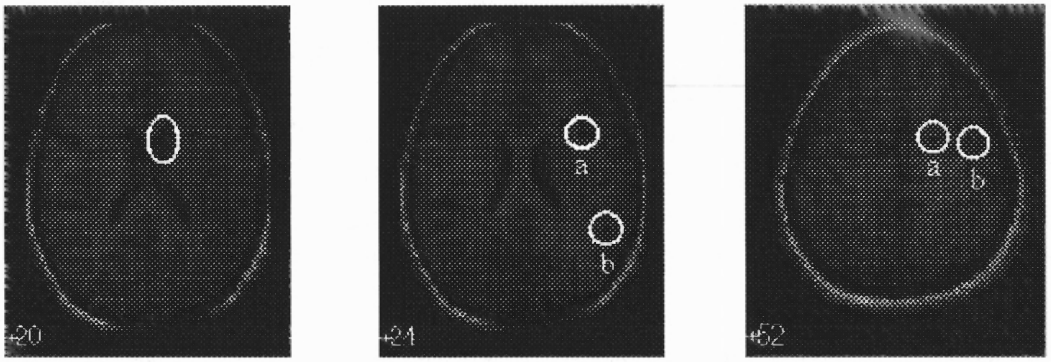

Caudate

a: Inferior Frontal Gyrus
b: Parietal Cortex

a: Middle Frontal Gyrus
b: Precentral Gyrus

Figure 4.4 Activity for the test of sensitivity for a High Load held over a Short Rehearsal Period

CHAPTER 5

DISCUSSION

5.1 Current Results

Baddeley [1] proposed a model of verbal working memory that consists of multiple components. Verbal information enters the temporary storage buffer where it is rehearsed until necessary manipulations occur, or the information is no longer needed. Smith et al. [3] proposed a set of neural substrates associated with the different components of Baddeley's model. After entering the system, phonological information is maintained in the storage buffer by means of subvocal rehearsal, i.e. the person silently repeats the information. This process involves Broca's Area, BA 44, inferior and superior aspects of BA 6. The proposed rehearsal circuit appeared to be involved in both main effects tested in this study (of memory load and length of rehearsal period).

All four-task conditions required rehearsal of stored information. If there were no increased involvement of these regions when the memory load increased or the rehearsal period increased, no activation in these regions would be expected. This is due to similar levels of activation not surviving the subtractions employed by the analysis. However, the fact that regions show an increase in activation in the main effect tests, tells that their involvement is related to the increased demands on the sub-systems.

Multiple regions of BA 6 are involved in the subvocal rehearsal of information. Both main effect tests revealed activity in bilateral medial frontal gyri and bilateral superior frontal gyri. The rehearsal sub component of working memory is therefore active

in the task. The test for sensitivity to high loads held over a long rehearsal period revealed activity in the right medial frontal gyrus and the left precentral gyrus. The test for sensitivity to high memory load held over a short rehearsal period revealed activity in the right precentral gyrus.

The DLPFC was evoked in this experiment by the main effect of rehearsal period and not by the main effect of memory load. Baddeley [1] hypothesized that there is a threshold on the number of items placed into memory storage to elucidate central executive activation. Rypma et al. [6] address this hypothesis and apply it to their study to explain their lack of DLPFC involvement in their main effect of memory load. In other words, they feel that they did not use enough letters in their memory load condition. Barch et al. [7] found left sided activation in the DLPFC while testing for a main effect of rehearsal period. The findings in this region are bilateral with the right hemisphere greater than the left. The experiments mentioned previously that use the n-back task also found activity in this region; they hypothesized this as being due to the increase in memory load. [4, 8] D'Esposito et al. [22] describe a range of involvements that the DLPFC may have in working memory. One result is that the DLPFC is recruited by active maintenance in working memory. The results support this view of DLPFC involvement.

The storage buffer of this system resides outside of the frontal regions in the parietal lobes (BA 40/7). Activation in the storage region BA 40 was evoked during the main effect of rehearsal period in the left hemisphere. This finding agrees with that of Barch et al. [7]. The increase in this region shows there is an effective relationship between the amount of activity and the length of time items are held in storage. Testing

for sensitivity to high memory loads held over a long rehearsal period revealed activity in right hemisphere BA 7. This right hemisphere activity is evident in the two n-back studies [4, 8]. The confound of memory load and rehearsal period in the n-back task may be the cause of their finding activity in this region.

The caudate body, implicated in other working memory studies [6, 23], is activated to a minimal extent when the memory load increases. The interaction test for sensitivity to a high memory load retained over a short rehearsal period; however, revealed activation in the caudate body to a greater extent. Bilateral cingulate gyri activation and right hemisphere anterior cingulate gyrus were also active during the main effect of delay. The bilateral cingulate gyrus activation was also evident in the main effect of load but to a lesser extent.

Although the cerebellum and thalamus are not included in the hypothesized regions of interest, their evocation by the experiment deserves some discussion. Andreasen et al. [24] investigated and summarized the cerebellum's involvement in cognitive tasks. Their hypothesis, based on anatomical studies and mounting functional imaging evidence, is that the cerebellum is involved in episodic memory retrieval. The results of testing for conscious recall of an episodic memory involved a network of activations. This network involved cellebellar, medial frontal, medial dorsal thalamus, parietal, and anterior cingulate activations. They hypothesize that these regions of activation represent a network that may represent a feedback loop that links cortical regions to the cerebellum through the thalamus. This network may be engaged in the planning, initiating and coordination of conscious retrieval.

The tests for the main effect of memory load showed activation in bilateral cerebellum, bilateral thalamus, anterior cingulate and medial frontal regions with no activation in parietal regions. If this hypothesized network were indeed activated, the parietal region may not be activated due to its involvement in referencing visuospatial associative memories [24] and not verbal memories.

5.2 Methods for Analysis

The methods of interpreting the results of this study are more revealing. The data were analyzed using SPM99 where the output is a statistical parametric map. Shown on such a map are the clusters of activation. A cluster as used here is a contiguous set of voxels having significance greater than the threshold. One way of reporting a cluster of activation is to report the location of the cluster's maxima. As discussed above this report tells nothing of the extent of the activated cluster. Often reported in the literature is a summary table of the maxima of the activated clusters and their anatomical regions. Some papers go beyond this and report the number of activated voxels in a cluster. This does not mean that the number of voxels in this cluster all exist in the anatomical region represented by the maxima. The cluster may be focally contained within the anatomical region defined by the maxima; however, there is a greater chance that the cluster extends into the anatomical regions' neighbors. Just knowing the maxima and the number of voxels contained in the cluster offer none of this insight.

A more revealing method of reporting results is that here. Taking all voxels within a cluster into account when reporting activation gives a better description of the extent of the clusters. This method offers the number of activated voxels in each brain region (as

described in the atlas of Talairach and Tournoux) contained in the cluster and not only the clusters' maxima.

The task used here is quite similar to that used by D'Espostio et al. [22]; however, the methods of analyses between the data are quite different. The aim of this study was to show the benefits of a factorial design in the context of a verbal working memory experiment and not the short time scale responses occurring because of this task. There are some critiques of a blocked design such as that used here and addressed by D'Esposito et al. [22]. These critiques are that the temporal resolution of a blocked design is temporally poor and ill suited for direct measure of processes operating on the order of seconds and milliseconds. This is correct and the design is not in a position to make direct measures of short time scale processes. The timing parameters of the task do allow for analysis of the data in a fashion similar to that of D'Esposito, [22, 25] which would allow for investigation of the processes operating on short time scales. For this experiment, a design was chosen that was more parsimonious and allowed for a greater ease of interpretation. The second critique presented, addresses the issue of pure insertion. This is not an issue for this experiment due to the subtractions performed. Subtraction is used to make comparisons between conditions; however, there is not a "control" task being subtracted out, only different levels of the manipulated factors. All conditions of this experiment involve the same cognitive components to different levels; therefore, "pure insertion" [9] is not an assumption made here.

5.3 Future Directions

This design has demonstrated its ability to reveal activation in all of the hypothesized regions. Knowing this and now having a greater understanding of verbal working memory, a step forward with more complicated analyses such as approaches taken by D'Esposito et al. [22] is reasonable. Their methods of analyses allow them to test for differences in the neural processes taking place when different numbers of items are encoded. The difference between this approach and the approach taken in the current study is that the encoding phase is that time when the items are first presented, and first entered into the storage system before rehearsal of the stored items. Their analyses also allow for testing between the beginning and the end of the rehearsal period. They are able to investigate differences occurring across this time interval. The design is analyzed in "blocks," that is the encoding phase, the entire rehearsal phase and the retrieval phase of the verbal working memory process are collapsed across. This allowed us easier interpretation of results.

In an experiment similar to this one, Nystrom et al. [26] describe the nature of Broca's Area involvement. This study showed activation with different time courses between long rehearsal periods and short rehearsal periods. They also show that activity in this region increases with an increase in memory load. The nature of the potentially different responses was not investigated in this study. This sort of time course investigation may offer valuable information into the nature of the involvement for regions involved in performing a verbal working memory task.

5.4 Flaws in the Current Design

One flaw in the implementation of the task concerns timing issues. The rate of presentation of letters in the initial block of letters varied depending on whether two or five letters were presented. Presentation of letters occurred over a five second period regardless of whether it was two or five letters. For five letters the rate was one letter every second and for two letters the rate was one letter every two and a half seconds. This difference in presentation rate may enter unnecessary confounds into the data. A better method of stimulus presentation is with a fixed rate of presentation regardless of the number of letters presented.

Another issue in this experiment is the lack of counter balancing. Since the presentation of different trial types was a fixed pattern, ordering effects may occur. For instance, there may be an effect of the presentation of a high load / long rehearsal interval on the following presentation a low load / short rehearsal period presentation. Since these two trials always occurred is this order, there was no way of accounting for any effect these trial types may have had on one another. An improved design would randomize the order of presentation of different trial types to average out any ordering effects.

CHAPTER 6

CONCLUSIONS

The results of this study show the DLPFC involved with an increase in memory rehearsal, agreeing with D'Esposito et al.'s [19] discussion of this region and the results of Cohen et al. [8]. This region also showed sensitivity to a high load held over a short rehearsal period. This may indicate that rehearsing a high memory load for only a short period of time calls for greater resource allocation and executive processes. The interaction tests show the involvement of BA 6 and 7 in working memory may be more complex than revealed in previous findings. The use of a two-factor design has proven effective in investigating verbal working memory. The design allowed for placement of demands on the verbal working memory system that elucidated responses in previously detected brain regions for similar tasks. The interaction tests furthermore allowed for further insight into the working memory sub components.

APPENDIX A

JRSTREAMTAL.M

This function extracts the x, y, z coordinates from the SPM99 software and saves them to a file.

%function jrstreamTAL.m

```
%
%This is a script which takes all the voxels activated in your glass brain and writes them %out to a file or files. The purpose is for preparing your data to be sent to the Talairach %Daemon. It is for this reason that there is a size limit on the extracted file size of 10000 %entries. The Talairach Daemon stand alone program imposes this file size limit. This %script also employs the MNI to Talairach coordinates program of Matt Brett.
%
%Jason Steffener v1.1
%July 19, 2001
%
a=SPM.XYZmm';
b=mni2tal(a);
n=size(b,1);
m=n/10000;
m=ceil(m);
P=SPM.title;
q=findstr(P,' ');
for i=1:length(q)
  P(q(i))='_';
end
for j=1:m
P=cat(2,P,'_k',num2str(SPM.k),'_T',num2str(SPM.u),'_',num2str(j),'.txt')
fid=fopen(P,'a');
for i=(j-1)*10000+1:j*10000
  c=round(b(i,:));
  fprintf(fid,'%2.0f     %2.0f  %2.0f\n',c);
end
status=fclose(fid);
clear a b n P q c
```

APPENDIX B

ROITAL.M

This function summarizes the results of the Talairach Daemon and creates a table showing the number of activated voxels in each different region of the brain.

%function roital.m

```
%
%This script opens a text file which is the output of the Talairach Daemon returned by
%the Daemon and returns a comma delimitated text file with each row being a different
%brain region and the final number being the total number of activated voxels per brain
%region.
%
%Jason Steffener
%March 25, 2001
%
amount=[1];
in=spm_get(1,'*.txt','Choose the Talairach file')
file=textread(in,'%s','delimiter','\n','whitespace',");
final={'Level1  ,Level2  ,Level3  ,Level4  ,Level5   '};
[k,l]=size(file);
for i=1:k
  tmp=char(file(i));
        commas=findstr(',',tmp);
        [n,m]=size(tmp);
  tmp2=tmp(commas(4)+1:m);
        bool=strcmp(final,tmp2);
if bool==0
  [o,p]=size(final);
  final{p+1}=tmp2;
  amount=[amount,1];
else
  position=find(bool);
  amount(position)=amount(position)+1;
end;
end
slash=findstr('\',in);
dot=findstr('.',in);
out=cat(2,'total_',in(max(slash)+1:max(dot)-1),'.txt')
fid=fopen(out,'a');
[m,n]=size(final);
for j=1:n
```

```
  temp=final{j};
  temp2=cat(2,temp,',',num2str(amount(j)));
  fprintf(fid,temp2);
  fprintf(fid,'\n');
end
status=fclose(fid);
clear
```

APPENDIX C

MERGE.M

This function merges two tables from the roital.m and allows for comparison of the results

%function merge.m

```
%Jason Steffener
%May 3, 2001
%This program merges two files together.
%This program takes the results of two summarized Talairach results files and merges
%them together. It shows brain regions followed by the number of voxels in each region
%in each of the two files you give it. I use this to compare the results from two different
%contrasts. If these instructions are confusing, use it and it will be evident.
%
amount=[1];
in=spm_get(2,'*.txt','Choose Two Talairach Result files to merge')
in1=textread(in(1,:),'%s','delimiter','\n','whitespace','');
in2=textread(in(2,:),'%s','delimiter','\n','whitespace','');
[a]=size(in1,1);
[b]=size(in2,1);
  file1=in1;
        file2=in2;
[k1,l1]=size(file1);
[k2,l2]=size(file2);
f1sum=(zeros(k1,1));
f1=char(zeros(k1,100));
for i=1:k1       %create array of file1 sums
  tmp1=char(file1(i));%take line(i) of file
  if size(tmp1,2)~=0   %This checks for empty lines
        commas1=findstr(',',tmp1);
        [n1,m1]=size(tmp1);
         tmp1t=tmp1(max(commas1)+1:m1);
         t=size(tmp1t,2);
         f1sum(i)=str2num(tmp1t);
         tmp1s=tmp1(1:max(commas1)-1);
         s=size(tmp1s,2);
         f1(i,1:s)=(tmp1s);
  end   %We no have 2 char arrays, one for the areas in the bigger TD file
end     %and one containing the sums of the locations
f2sum=(zeros(k2,1));
f2=char(zeros(k2,100));
```

```
for i=1:k2                    %create array of file1 sums
  tmp2=char(file2(i));        %take line(i) of file
  if size(tmp2,2)~=0
        commas2=findstr(',',tmp2);
        [n2,m2]=size(tmp2);
        tmp2t=tmp2(max(commas2)+1:m2);
        t=size(tmp2t,2);
        f2sum(i)=str2num(tmp2(max(commas2)+1:m2));
        tmp2s=tmp2(1:max(commas2)-1);
        s=size(tmp2s,2);
        f2(i,1:s)=(tmp2s);
  end
end             %What we now have is four have arrays, 2 for each input file.
 count=k1;
 outfile=f1;
 outfilecount=f1sum;
 for k=1:k2     %loop over file2
  for j=1:k1    %loop over file1
   bool=strcmp(f1(j,:),f2(k,:));
   if bool==1
        outfilecount(j,2)=f2sum(k);
        break
   end
  end
  if bool==0
        count=count+1;
        outfile(count,:)=f2(k,:);
        outfilecount(count,2)=f2sum(k);
  end
end
m=size(outfile,1);
out='mergeout.txt'
fid=fopen(out,'a');
fprintf(fid,',,,,,');
slash=findstr('\',in(1,:));
dot=findstr('.',in(1,:));
fprintf(fid,in(1,max(slash)+1:dot-1));
fprintf(fid,',');
slash=findstr('\',in(2,:));
dot=findstr('.',in(2,:));
fprintf(fid,in(2,max(slash)+1:dot-1));
fprintf(fid,'\n');
for j=1:m
  temp=deblank(outfile(j,:));
  temp3a=outfilecount(j,1);
  temp3b=outfilecount(j,2);
```

```
  temp2=cat(2,temp,',',num2str(temp3a),',',num2str(temp3b));
  fprintf(fid,temp2);
  fprintf(fid,'\n');
end
status=fclose(fid);
disp('Done!!');
clear
```

REFERENCES

1. Baddeley, A., *Working Memory.* Science, 1992. **255**: p. 556-559.

2. Henson, R.N.A., N. Burgess, and C.D. Frith, *Recoding, storage, rehearsal and grouping in verbal short-term memory: an fMRI study.* Neuropsychologia, 2000. **38**: p. 426-440.

3. Smith, E.E., et al., *Components of verbal working memory: Evidence from Neuroimaging.* Proceeding of the National Academy of Sciences, USA, 1998. **95**: p. 876-882.

4. Braver, T.S., et al., *A Parametric Study of Prefrontal Cortex Involvement in Human Working Memory.* NeuroImage, 1997. **5**: p. 49-62.

5. Honey, G.D., E.T. Bullmore, and T. Sharma, *Prolonged Reaction Time to a Verbal Working Memory Task Predicts Increased Power of Posterior Parietal Cortical Activation.* Neuroimage, 2000. **12**: p. 495-503.

6. Rypma, B., et al., *Load-Dependent Roles of Frontal Brain Regions in the Maintenance of Working Memory.* NeuroImage, 1999. **9**: p. 216-226.

7. Barch, D.M., et al., *Dissociating working memory from task difficulty in human prefrontal cortex.* Neuropsychologia, 1997. **35**(10): p. 1372-1380.

8. Cohen, J.D., et al., *Temporal Dynamics of Brain activation during a working memory task.* Nature, 1997. **386**: p. 604.

9. Friston, K.J., et al., *The Trouble with Cognitive Subtraction.* Neuroimage, 1996. **4**: p. 97-104.

10. Bandettini, P.A., R.M. Birn, and K.M. Donahue, *Functional MRI, Background, Methodology, Limits, and Implementation*, in *Handbook of Psychophysiology*, J.T. Cacioppo, L.G. Tassinary, and G.G. Bernston, Editors. 2000, Cambridge University Press. p. 978-1014.

11. Ogawa, S., et al., *Intrinsic signal changes accompanying sensory stimulation: Functional brain mapping with magnetic resonance imaging.* Proc. Natl. Acad. Sci., 1992. **89**: p. 5951-5955.

12. Kwong, K.K., et al., *Dynamic magnetic resonance imaging of human brain activity during primary sensory stimulation.* Proc. Natl. Acad. Sci., 1992. **89**(12): p. 5675-9.

13. Coull, J.T., et al., *Orienting Attention in time: behavioral and neuroanatomical distinction between exogenous and endogenous shifts.* Neuropsychologia, 2000. **38**: p. 808-819.

14. Friston, K.J., et al., *Statistical Parametric Mapping in functional imaging: A general linear approach.* Human Brain Mapping, 1995. **2**: p. 189-210.

15. Talairach, J. and P. Tournoux, *Co-Planar Stereotaxtic Atlas of the Human Brain.* 1988: Thieme, New York.

16. Friston, K.J., et al., *Spatial registration and normalization of images.* Human Brain Mapping, 1995. **2**: p. 165-189.

17. Ashburner, J. and K.J. Friston, *Multimodal Image Coregistration and Partitioning - a Unified Framework.* Neuroimage, 1997. **6**: p. 209-217.

18. Ashburner, J. and K.J. Friston, *Nonlinear Spatial Normalization using Basis Functions.* Human Brain Mapping, 1999. 7(4): p. 254-266.

19. Glover, G.H., *Deconvolution of Impluse Response in Event-Related BOLD fMRI.* Neuroimage, 1999. **9**: p. 416-429.

20. Holmes, A.P. and K.J. Friston, *Generalisability, Random Effects And Population Inference.*

21. Brett, M., K. Christoff, and J. Lancaster, *Using the Talairach atlas with the MNI template.* 2001.

22. D'Esposito, M., B.R. Postle, and B. Rypma, *Prefrontal cortical contributions to working memory: evidence from event-related fMRI studies.* Experimental Brain Research, 2000. **133**: p. 3-11.

23. Postle, B.R. and M. D'Esposito, *Dissociation of human caudate nucleus activity in spatial and nonspatial working memory: an event-related fMRI study.* Cognitive Brain Research, 1999. **8**: p. 107-115.

24. Andreasen, N.C., et al., *The Cerebellum Plays a Role in Conscious Episodic Memory Retrieval.* Human Brain Mapping, 1999. **8**: p. 226-234.

25. D'Esposito, M., et al., *Maintenance versus Manipulation of Information Held in Working Memory Memory: An Event Related fMRI Study.* Brain and Cognition, 1999. **41**: p. 66-86.

26. Nystrom, L.E., et al., *Dynamics of fMRI: Brocas are activation reflects independent effects of duration and intensity of working memory processes.* Neuroimage, 1998. 7(S7).